NJC

LETTER

View Article Online
View Journal



Cite this: DOI: 10.1039/c9nj02351h

Received 7th May 2019,
Accepted 3rd August 2019

DOI: 10.1039/c9nj02351h

rsc.li/njc



# Improving the photo-cathodic properties of $TiO_2$ nano-structures with graphdiynes†

Vivek Ramakrishnan, ‡ Hyun Kim and Beelyong Yang *

**Graphdiyne (GD) nanoscale films were initially synthesised on copper foils and its oxide form, GD oxide (GDO) obtained by subsequent oxidation of purified GD. Hybrid nanocomposites of both GD and GDO with hydrothermally grown $TiO_2$ nanorods were prepared by various methods, and their photo-electrochemical (PEC) properties were studied. Both the systems were found to perform as an improved photo-cathodic material with GDO found to have superior PEC properties.**

Metal oxide nanostructures and their hybrid materials have been widely used for energy production mainly in the area of electro- and photo-catalysts or both combined for energy power conversion.[1–6] Researchers are engineering inorganic–organic hybrid systems, in such a way to achieve maximum efficiency by combining two or more systems to get superior properties. One of the potential candidates in such systems is Titanium dioxide ($TiO_2$) based nanostructures which have been well studied in the field of photocatalysis. It's chemical stability, low cost, abundance and favourable band edge alignment with water redox potentials make them a desirable contender as photo-anodes for water oxidation. Among the scientific community, there have been numerous reports for enhancing the photo-cathodic activity of metal oxide nanostructures with metal-free systems (polymers, nitrides *etc.*) and also for improving the photocathodic activity of $TiO_2$ nanostructures (Table S1, ESI†). It's always desirable to make a tandem nanostructure which can be active for photo-cathodic and anodic activation of water by coupling with a suitable material and it is highly advantageous to have if it's a metal-free system like graphene or its derivatives. Following enormous 'activity' of graphene (GR), the pathway for a unique series of two-dimensional layered materials was introduced into the research world, namely, graphyne, graphdiyne (GD), graphone, and graphane.[7–10]

GD is one of the most stable among various human made diacetylenic carbon allotropes studied to date and therefore one of the most synthetically approachable. Similar to GR, GD is also a two-dimensional planar structured material which has several properties to improve the photocatalytic performance of $TiO_2$, including large surface area and high electron mobility.[8,11] Low bandgap combined with high charge carrier mobility are very desirable characteristics which make them impending candidates in photocatalytic water splitting.

GD is found to be a semiconductor and is highly stable at elevated temperatures even up to 800 °C. These materials can be interconverted to other nanomeric forms possessing superior properties such as increased electron mobility and conductivity. After a hydrothermal reaction, the diacetylenic linkage of GD can partly transform into a two-dimensional π-conjugated structure favourable for electronic transmission. In addition, these materials can be used to expand the light absorption range and suppress electron–hole recombination when linked with $TiO_2$ like metal oxides.[12,13]

Recently, GD and GD oxide (GDO) based photocatalysts have been reported in combination with semiconductors having a larger bandgap by several research groups. The various forms of GD like nanoparticle composites, nanoflakes and nanowires have been reported to show superior photocatalytic properties by depositing on semiconducting metal oxides.[14–18]

In this work, we have synthesised GD and GDO and nano-structure composites with $TiO_2$ (Fig. 1) were further prepared and photo-electrochemical (PEC) studies were performed. GD films on copper foils were synthesised by *in situ* growth according to the reported method by G. Li *et al.*[11] (ESI†) with hexaethynylbenzene monomer as the starting material. The as-prepared GD on copper foil was transformed into GD powder by immersing in trichloro-butane followed by sonication after purifying with various solvent mixtures (ESI†).

The as-prepared GD films were characterised by Raman spectroscopy. As shown in Fig. 2a, spectra display four peaks

*School of Advanced Materials and System Engineering, Kumoh National of Institute of Technology, Yangho-dong, Gumi-si, Gyeongsangbuk-do, Korea.*
*E-mail: blyang@kumoh.ac.kr*

† Electronic supplementary information (ESI) available. See DOI: 10.1039/c9nj02351h

‡ Present address: National Solar Energy Centre, Ben-Gurion University of the Negev, Sede Boqer Campus, 84990 Israel.

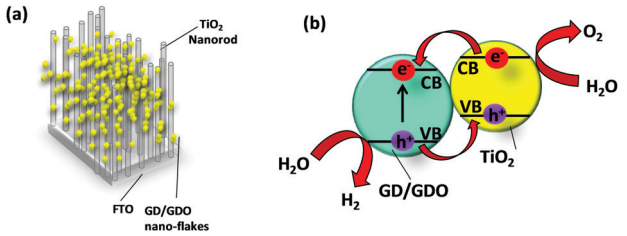


Fig. 1 (a) A schematic diagram of the GD ~ GDO/$TiO_2$ nanostructure and (b) band diagram electron–hole movement.

at 1380 $cm^{-1}$, 1570 $cm^{-1}$, ~1940 $cm^{-1}$ (broad) and ~2190 $cm^{-1}$ (broad) respectively.[19,20] The prominent peak at 1380 $cm^{-1}$ and 1570 $cm^{-1}$ corresponds to the vibration of $sp^2$ carbon domains in aromatic rings and in-phase stretching vibration of $sp^2$ carbon domains in aromatic rings. Both the peaks are deviated from the graphitic peaks, where the former one (D band) is blue shifted and the latter one (D band) is red shifted compared to the G band of graphite (1575 $cm^{-1}$). The intensity ratio of the D to G band is calculated to be ~0.70, indicating the multilayer nature of the GD films with high order and low defects. The broad and comparatively weaker peaks observed at a higher wavenumber region are attributed to the acetylenic linkages (~1940 and ~2190 $cm^{-1}$).

To further prove the GD formation on Cu foil and crystalline behaviour, X-ray diffraction (XRD) analysis was performed, as shown in Fig. 2b. The peak at 44.7° represents the GD whereas the rest of the peaks arise due to Cu foil matching very well, with and without GD.[11,17,19] The above fact is further supported by the high-resolution transmission electron microscopy (HRTEM). Fig. S1a in the ESI† depicts the SAED (Fig. S1b–d, ESI†) and lattice fringe corresponding to GD consistent with the XRD measurements. The chemical nature of the GD films synthesised was further confirmed by Fourier transform infrared spectroscopy (FT-IR) analysis as well (Fig. S1e, ESI†). The characteristic peaks (1590 and 2100 $cm^{-1}$) were identified attributed to aromatic and acetylenic systems.

The GDO powder samples were prepared by strong acid oxidation by a mixture of $H_2SO_4/HNO_3$ with $KMnO_4$ (ESI†).[16] We have tried to engineer hybrid samples of GD and GDO with $TiO_2$ nanorods by several processes (Table S2, ESI†), among which the hydrothermal route was found to be effective for PEC activity. Anchoring of GD/GDO on $TiO_2$ nanorods was carried out by one step (*in situ*) synthesis, *i.e.* the GD or GDO sample will be added along with standard growth of $TiO_2$ nanorods on FTO with varying weight percentages (ESI†).

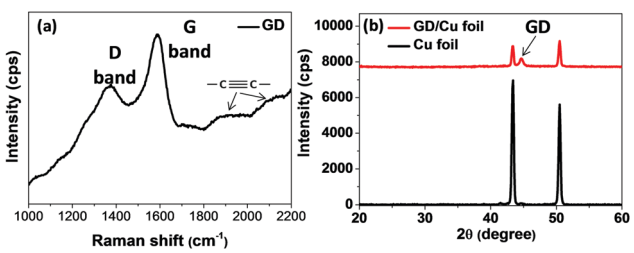


Fig. 2 (a) Raman spectra and (b) XRD analysis of synthesized GD.

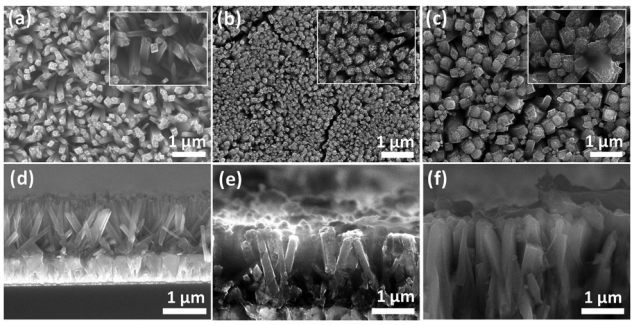


Fig. 3 FESEM images of (a) $TiO_2$, (b) GD/$TiO_2$ and (c) GDO/$TiO_2$ and (d–f) their respective vertical image analysis prepared by one step synthesis.

The surface morphology of the hybrid GD and GDO with $TiO_2$ is shown in Fig. 3 and compared with bare $TiO_2$ nanorods.

Horizontal images outline the gradual increase in the size of the nanorods from bare $TiO_2$ to GD and then to GDO incorporated hybrids. The vertical FESEM (Fig. 3d–f) analysis clearly outlines the growth of GD and its oxide on the nanorod structure.

HRTEM measurements of the GD/$TiO_2$ composite *in situ* (1 step method) also evidently mark the GD grafted $TiO_2$ nanorods (Fig. 4). The high-resolution image, Fig. 4c identifies both the GD and $TiO_2$ nanostructures marking the corresponding crystal planes of both components as can be interpreted from Fig. 4c. The SAED pattern also confirms the attachments of GD on the $TiO_2$ nanostructure as depicted in Fig. 4c. The formation of the hybrids prepared was further probed by XRD and FT-IR methods (Fig. S2b and c, ESI†). To further confirm the formation of the hybrid GD/$TiO_2$ and to understand the chemical and valence state, X-ray photoelectron spectroscopic measurements (XPS) were performed and compared with the reported data.[11,17,19,20] The survey

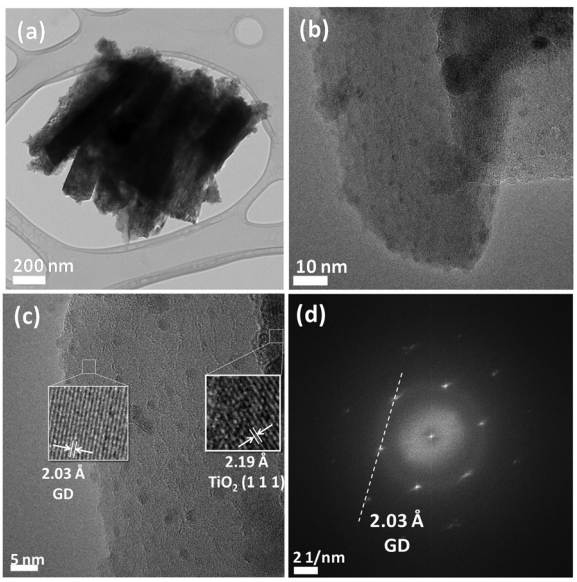


Fig. 4 (a) Low resolution and (b) high-resolution TEM analysis and (d) SAED pattern of GD/$TiO_2$ prepared by one step synthesis.

spectrum clearly shows the presence of C, Ti and O (Fig. S2d, ESI†). The C 1s peak in Fig. S2e (ESI†) is analysed and found to be composed of 4 states such as C–C ($sp^2$, 284.6 eV), C–C (sp, 285.9 eV), C–O (287.3 eV), and C═O (288.8 eV). The occurrence of characteristic peaks of Ti at 458.5 (Ti $2p_{3/2}$) and 464.3 eV (Ti $2p_{1/2}$) clearly suggests that $Ti^{4+}$ is the major valence state in the hybrid (Fig. S2f, ESI†). Before executing the PEC activity, preliminary photo-physical properties have been explored, such as UV-Visible spectral measurements. From Fig. S3 (ESI†), we can depict a small, distinct improvement towards the higher wavelength for the hybrids of GDO compared to bare $TiO_2$.

Photocurrent densities of the as-prepared $TiO_2$, GD/$TiO_2$ and GDO/$TiO_2$ by a 1 step process are measured and compared to the PEC activity among each other in a 0.1 M $Na_2SO_4$ aqueous solution under visible light (in addition, the PEC activity of hybrids prepared by other methods stated in Table S2 is shown in Fig. S4, ESI†). A photocurrent density of ~58 μA can be obtained at an applied potential of 0 V which was more than 10 times larger than bare $TiO_2$ (~5 μA), improving the photo-cathodic property of the nanostructure remarkably. Interestingly with the *in situ* preparative method, the PEC activity of the GD composite was not improved very much from that of bare $TiO_2$. As we prepared the GDO/$TiO_2$ composite by an *in situ* method, the effect of intercalation amount also has been taken into account as can be seen from Fig. 5b. A gradual increase in the PEC activity was shown when the weight percentage of the GDO is gradually increased from 1 to 10 to 100. The PEC activity was found to decrease with further increase in the loading amount of GDO to $TiO_2$ (Fig. S5a, ESI†). A photocurrent density of 0.24 mA is observed for a cathodic applied potential of 1 V. At 1 V, the enhancement factor was calculated to be ~30 times that of the bare $TiO_2$. The effect of varying light intensities was also studied on the most efficient sample (100 wt% GDO/$TiO_2$ – *in situ*). As shown in Fig. S5b (ESI†), we can descry a linear increase in the net photocurrent with an increase in the light intensity.

The stability of the GDO/$TiO_2$ hybrid sample was tested by applying a constant potential of −0.8 V under illumination in 0.1 M $Na_2SO_4$ aqueous solution (Fig. S6a, ESI†). The PEC stability of GDO/$TiO_2$ is further proved by characterisation before and after PEC measurements (Fig. S6b, ESI†). To optimise and obtain maximum PEC activity, *ex situ* (2 step) synthesis of GD/GDO on $TiO_2$ nanorods was carried out (ESI†). In this particular case, the GD or GDO sample would be grown in a second step following the growth of $TiO_2$ nanorods on FTO by a hydrothermal method. The PEC activity was not high enough compared to that of the *in situ* prepared nanostructures (Fig. S7, ESI†). But the photocurrent density of the GD incorporated nanostructure was heavily increased compared to the *in situ* process. In contrast, the GDO integrated $TiO_2$ nanocomposite showed fluctuating behaviour and showed decreased activity (Fig. S8, ESI†) compared to its *in situ* counterpart. In any case, the amount of GD was not found to have enough influence on the PEC activity (Fig. S9, ESI†).

The improved photo-cathodic activity is attributed to the combined effect of GD and its oxide on $TiO_2$, unlike the graphene or its derivatives where it may improve the anodic activity.[21,22] Recently, researchers have tried to improve the photo-cathodic activity coupling with GD and our system shows comparable or even better photo-current density reported so far to the best of our knowledge.[15,23] In the 1 step *in situ* growth, there will be an efficient interaction between $TiO_2$ and GDO. With the introduction of lattice oxygen, the interlinkage between the metal oxide and oxidic GD enhances, causing better charge transfer leading to improved PEC activity. Such kind of interaction is less for GD where it has less polarity and minor interaction with the titanium precursors in the polar reaction medium. The charge transfer phenomenon could be very effective by *in situ* synthesis where there can be direct Ti–C linkage.[24] Nevertheless, the corresponding interaction will be less prominent for *ex situ* derived hybrids. This kind of advantage for *in situ* methods has been explored for hybrid nanostructure preparation with enhanced photoactivity.[24–27]

In summary, a metal-free carbon material GD/GDO has been infused with $TiO_2$ nanostructures with enhanced photo-cathodic activity for the first time. *In situ* and *ex situ* introduction of GD and its oxide caused improvement in the PEC activity, with the former favouring the GDO hybrid and the latter favouring the GD. Hole transportation and improved photocurrent was established by the strong π–π interactions between GD/GDO and $TiO_2$. GDO/$TiO_2$ photocathodes prepared by the *in situ* method showed an enhancement factor of 10 times the photocurrent density even for a bias-free state (0 V) compared to bare $TiO_2$. This study paves a new way to introduce GD and its oxides as a promising candidate in improving the photo-cathodic activity of well-known photo-anodes by which tandem nanostructures could be developed for efficient solar-to-fuel conversion. Systems with a tandem nanostructure of GD/GDO for PEC as well as gas evolution studies are in progress for a better understanding of the activity of the catalyst.

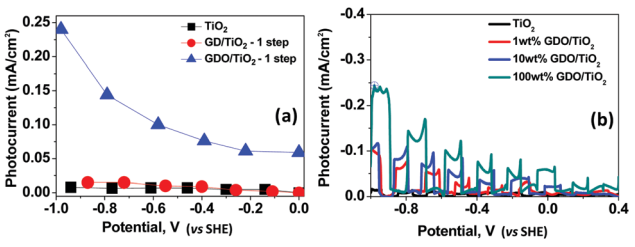


Fig. 5 (a) Comparison of the photocurrent density–voltage diagram of GD/$TiO_2$ and GDO/$TiO_2$ nanostructures prepared by 1 step hydrothermal synthesis and $TiO_2$ nanorods on FTO in 0.1 M $Na_2SO_4$ aqueous solution with visible light and (b) with varying weight percentage of GDO with $TiO_2$.

## Conflicts of interest

There are no conflicts to declare.

## Acknowledgements

This research was supported by the Space Core Technology Development Programme through the National Research

Foundation of Korea (NRF) funded by the Ministry of Education Science and Technology (MEST) (2017M1A3A3A02016666). The authors would like to acknowledge Prof. Iris Visoly-Fisher and Ilse Katz Institute for Nanoscale Science and Technology (Ben-Gurion University of the Negev, Israel) for extending XPS and additional PEC measurements.

## Notes and references

1 A. A. Ismail and D. W. Bahnemann, *Sol. Energy Mater. Sol. Cells*, 2014, **128**, 85–101.
2 K. Maeda and K. Domen, *J. Phys. Chem. Lett.*, 2010, **1**, 2655–2661.
3 A. Kudo and Y. Miseki, *Chem. Soc. Rev.*, 2009, **38**, 253–278.
4 S. J. Moniz, S. A. Shevlin, D. J. Martin, Z.-X. Guo and J. Tang, *Energy Environ. Sci.*, 2015, **8**, 731–759.
5 V. Ramakrishnan, H. Kim, J. Park and B. Yang, *RSC Adv.*, 2016, **6**, 9789–9795.
6 V. Ramakrishnan, C. Alex, A. N. Nair and N. S. John, *Chem. – Eur. J.*, 2018, **24**, 18003–18011.
7 Q. Peng, A. K. Dearden, J. Crean, L. Han, S. Liu, X. Wen and S. De, *Nanotechnol., Sci. Appl.*, 2014, **7**, 1–29.
8 K. Srinivasu and S. K. Ghosh, *J. Phys. Chem. C*, 2012, **116**, 5951–5956.
9 F. Diederich, *Nature*, 1994, **369**, 199–207.
10 Y. Zhang, T.-T. Tang, C. Girit, Z. Hao, M. C. Martin, A. Zettl, M. F. Crommie, Y. R. Shen and F. Wang, *Nature*, 2009, **459**, 820–823.
11 G. Li, Y. Li, H. Liu, Y. Guo, Y. Li and D. Zhu, *Chem. Commun.*, 2010, **46**, 3256–3258.
12 S. Thangavel, K. Krishnamoorthy, V. Krishnaswamy, N. Raju, S. J. Kim and G. Venugopal, *J. Phys. Chem. C*, 2015, **119**, 22057–22065.
13 S. Wang, L. Yi, J. E. Halpert, X. Lai, Y. Liu, H. Cao, R. Yu, D. Wang and Y. Li, *Small*, 2012, **8**, 265–271.
14 K. Krishnamoorthy, S. Thangavel, J. C. Veetil, N. Raju, G. Venugopal and S. J. Kim, *Int. J. Hydrogen Energy*, 2016, **41**, 1672–1678.
15 J. Li, X. Gao, B. Liu, Q. Feng, X.-B. Li, M.-Y. Huang, Z. Liu, J. Zhang, C.-H. Tung and L.-Z. Wu, *J. Am. Chem. Soc.*, 2016, **138**, 3954–3957.
16 H. Qi, P. Yu, Y. Wang, G. Han, H. Liu, Y. Yi, Y. Li and L. Mao, *J. Am. Chem. Soc.*, 2015, **137**, 5260–5263.
17 N. Yang, Y. Liu, H. Wen, Z. Tang, H. Zhao, Y. Li and D. Wang, *ACS Nano*, 2013, **7**, 1504–1512.
18 X. Zhang, M. Zhu, P. Chen, Y. Li, H. Liu, Y. Li and M. Liu, *Phys. Chem. Chem. Phys.*, 2015, **17**, 1217–1225.
19 Z. Lin, G. Liu, Y. Zheng, Y. Lin and Z. Huang, *J. Mater. Chem. A*, 2018, **6**, 22655–22661.
20 X. Gao, H. Ren, J. Zhou, R. Du, C. Yin, R. Liu, H. Peng, L. Tong, Z. Liu and J. Zhang, *Chem. Mater.*, 2017, **29**, 5777–5781.
21 F. Ning, M. Shao, S. Xu, Y. Fu, R. Zhang, M. Wei, D. G. Evans and X. Duan, *Energy Environ. Sci.*, 2016, **9**, 2633–2643.
22 C. N. Van, N. T. Hai, J. Olejnicek, P. Ksirova, M. Kohout, M. Dvorakova, P. Van Hao, P. N. Hong, M. C. Tran and D. Van Thanh, *Mater. Lett.*, 2018, **213**, 109–113.
23 T. Zhang, Y. Hou, V. Dzhagan, Z. Liao, G. Chai, M. Löffler, D. Olianas, A. Milani, S. Xu and M. Tommasini, *Nat. Commun.*, 2018, **9**, 1140.
24 Z. Lu, L. Zeng, W. Song, Z. Qin, D. Zeng and C. Xie, *Appl. Catal., B*, 2017, **202**, 489–499.
25 N. Jaafar, A. Jalil, S. Triwahyono, J. Efendi, R. Mukti, R. Jusoh, N. Jusoh, A. Karim, N. Salleh and V. Suendo, *Appl. Surf. Sci.*, 2015, **338**, 75–84.
26 Z. Liu, P. Fang, F. Liu, Y. Zhang, X. Liu, D. Lu, D. Li and S. Wang, *Appl. Surf. Sci.*, 2014, **305**, 459–465.
27 H. Zhu, D. Chen, D. Yue, Z. Wang and H. Ding, *J. Nanopart. Res.*, 2014, **16**, 2632.

 